Thermomechanical modeling of the stabilization process for carbon fiber production

Jan Wolf[1,3]*, Romy Peters[1,3], Jonathan Mädler[2], Daniel S. Wolz[1,3], Thomas Behnisch[1,3], Mohsen Sadeghi Bogar[1,3], Leon Urbas[2], Maik Gude[1,3]

[1]TUD Dresden University of Technology, Institute of Lightweight Engineering and Polymer Technology, Holbeinstraße 3, 01062 Dresden, Germany

[2]TUD Dresden University of Technology, Chair of Process Control Systems & Process Systems Engineering Group, 01062 Dresden, Germany

[3]TUD Dresden University of Technology, Research Center Carbon Fibers Saxony, Holbeinstraße 3, 01307 Dresden, Germany

Abstract

Within carbon fiber manufacturing, stabilization process is the most time- and energy-intensive process, due to the complexity of chemical structure transformation. Therefore, optimization is strictly required to enable cost-efficient stabilization processes. Within this study, for the first time a hybrid semi-parametric model for continuous stabilization is developed to prognose stabilization progress and density of the stabilized fiber. The proposed model takes the process parameters, like dwell time, stabilization temperature and fiber stretching, as well as precursor properties, such as fiber density, into account. Finally, the proposed hybrid semi-parametric model offers a novel plant transferable optimization solution for model-based energy optimization in the stabilization process.

Keywords: hybrid modeling, polyacrylonitrile, stabilization

1 Introduction

Carbon fibers (CF) have been gaining importance in recent decades as reinforcing materials in various industries, such as aerospace, automotive, medical and other lightweight construction applications [1–6]. Compared to steel or other metals, these fibers offer advantages over conventional materials due to their low mass combined with higher tensile strength and Young's modulus. In addition, CF are also characterized by high electrical and thermal conductivity and high creep resistance [1, 3, 4, 7–11] , so they can be used to enhance the conductive properties of polymer composites [10, 11]. As a result, the demand for CF, is permanently increasing, 92000 t to 107000 t from 2021 to 2022 [12]. To meet the demand, CF is typically produced in large-scale industrial continuous plants up to 6000 tons per year to provide low-cost fibers at mass-scale [13]. At the same time for research and small batch purposes small production volumes are needed. These CF are specifically adapted in their properties to meet the individual applications, such as porosity and mechanical load bearing functions for structural energy storages [14] or novel CF produced from alternative, renewable polymer precursor materials such as lignin [5, 15]. The development of such CF typically requires multi-year development efforts to enable product robust, energy-optimized processes. Therefore, the development of a novel CF involves many time-consuming and costly experiments [16, 17]. Concurrent, the developed processes need to be adapted for the specifically production plant. This restrict the possibility of CF for small volume productions and could be overcome by transferable process modelling approaches, which allows a fast and reliable process transfer between individual small production volume plants.

The CF manufacturing consists of stabilization, carbonization and optional graphitization. Especially, the stabilization process is the most energy-intensive and complex process step in CF production [1, 2, 9, 15, 17]. Due to long dwell times, several changes in fiber structure through parallel chemical reactions, resp. cyclization, dehydrogenation, oxidation, evolve and predefine the final CF properties. Up to now optimization of stabilization with regard to fiber properties and energy consumption is mostly done by

empirical approaches. These approaches need to be re-run by process transfer to other stabilization plants. The efforts and number of required experiments could be reduced by using hybrid semi-parametric models for modeling the stabilization process, as they have the opportunity to only adapt the plant-specific model part. This could enable the production of multifunctional CF from novel precursors at low production volumes.

Several modeling approaches for stabilization process can be found in the literature, which are either based on parametric physical and chemical laws (white-box) or follow purely data-driven approaches (black-box) [8, 18–21]. However, both pure modeling approaches exhibit inaccuracies in their comprehensive simulation of the complex stabilization process. For black-box approaches these are poor extrapolation possibilities outside the trained parameter areas, while white-box approaches cannot represent the complex reaction correlations. Also, the known approaches focus only on the process parameters temperature and residence time [6, 14], while neglecting the mechanical stress on the fiber within the stabilization furnace. Therefore, the suggested hybrid semi-parametric model includes all plant independent process parameters and takes the stabilization key indicators, fiber density and stabilization degree, into account. Thus, the model will provide two output parameters, one being the resulting density of the stabilized fiber and the other being the relative cyclization index (RCI). The latter is used to index the stabilization progress as the cyclization reaction is part of the reaction chain which is fundamental for resulting mechanical properties. As well as there are known areas for fiber density (e.g. PAN 1.35-1.38 g cm^{-3} [22]) which ensure good mechanical properties in tensile strength or Young's modulus.

2 Modeling approaches

The proposed hybrid semi-parametric model consists of the parametric model part based on chemical mass balances and the artificial neural network (ANN). Fig 1 shows the structure of the feed-forward ANN

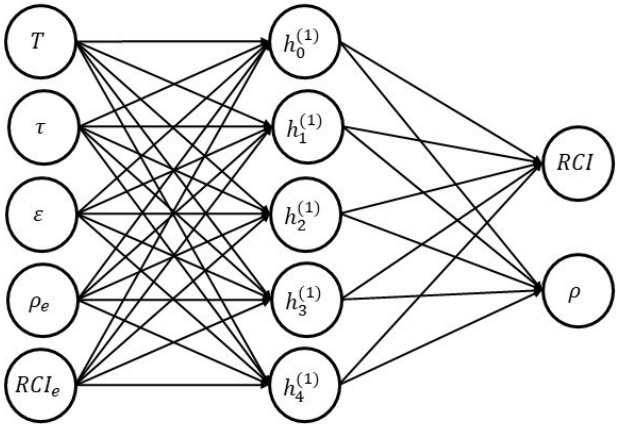

Figure 1 ANN used in the hybrid semi-parametric model with input parameters temperature T, residence time τ, fiber stretching, fiber density ρ_e and RCI_e, leading to the outputs of resulting fiber density and relative cyclization index

used for the simulation within the model. With the input parameters temperature, residence time, stretching and fiber density, the output parameters relative cyclization index and the density of the stabilized fiber are calculated. The parametric model part is derived from a mass balance for a continuous process according to Eq. (1). Where $\dot{n}$ is the mass flow rate of the not processed fiber portion, r is the reaction rate, and V_R is the reactor volume. By transformation, the residence time τ or the concentrations c are obtained as the ratio of V_R and the volumetric flow rate $\dot{V}$, which here is assumed to be constant, or the mass flow rates $\dot{n}$ (Eq. (2))

$$0 = \dot{n}_\mathrm{e} - \dot{n} - rV_R, \tag{1}$$

$$0 = c_e - c - kc\tau \,. \tag{2}$$

Here, the Arrhenius constant k provides the temperature influence for the modeling. Finally, Eq. (3) can be derived by introducing the cyclization index *RCI* as the progress index $\frac{c}{c_{e,1}} = (1 - RCI)$, while $c_{e,1}$ represents the concentration at the beginning of heating zone (HZ) 1 and RCI_e the cyclization index at the beginning of the current HZ

$$RCI = 1 - \frac{1 - RCI_e}{1 + k\tau} \,. \tag{3}$$

The fiber density ρ is calculated on the same mass balance approach. However, the mass flow rates of the product are substituted as the ratio of mass flows $\dot{m}$ and molar masses M (Eq. (4)). Further substitution of the mass flows as the product of volume flow and fiber density, brings the density into the equation. The fiber stretching ε can now be introduced as the ratio of the different fiber transport velocities u between the heating zones by substituting $\frac{\pi}{4} d^2 u$ for the volume flow $\dot{V}$

$$0 = \frac{\rho_e \dot{V}_e}{M} - \frac{\rho \dot{V}}{M} + k\tau \frac{\rho \dot{V}}{M} \,. \tag{4}$$

This gives Eq. (5), which contains D as an empirical factor for the ratio of the squares of the fiber diameters.

$$\rho = \frac{\rho_e D}{(1+\varepsilon)(1-k\tau)} \tag{5}$$

The total hybrid semi-parametric model follows a parallel setup with the ANN and parametric approach combined, which results in two outputs. The final output is chosen by a convex hull, raised by stabilization temperature, stabilization residence time and stabilization stretching. The structure of the stabilizing furnace used, with four HZs, is taken into account in the modeling in the form of a series of hybrid models. This model behavior corresponds to a stirred tank cascade and offers the opportunity to extend the model by more or less HZs.

Accordingly, four models are combined in the process system, shown in Fig. 2, with the resulting density of one model being used as the input parameter for the following one.

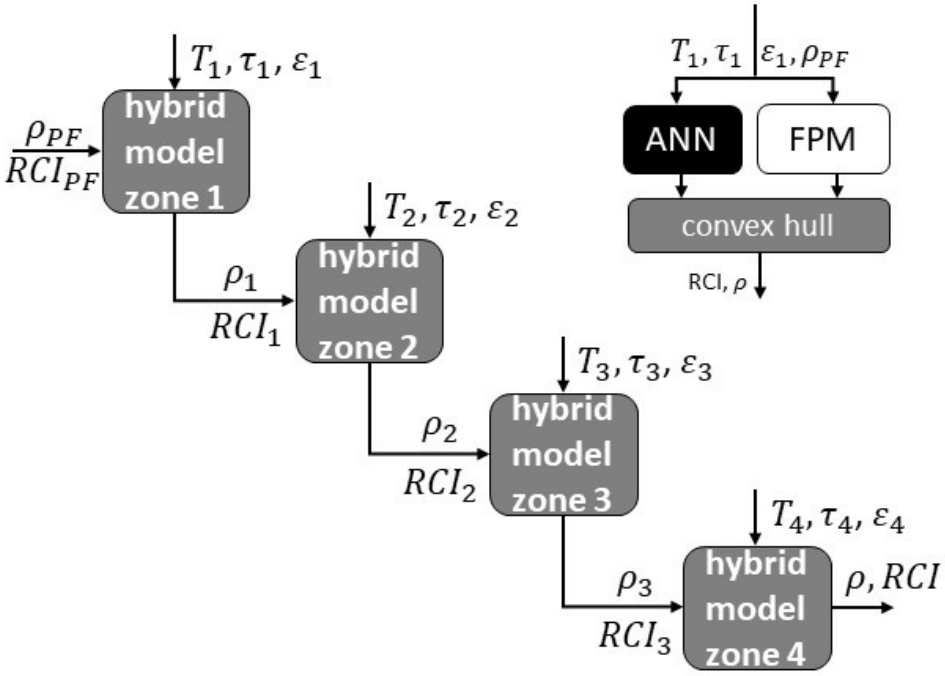

Figure 2 Four hybrid semi-parametric models connected due to the simulation of each HZ in the stabilization oven(left), parallel setup for the hybrid model consisting of an ANN, the parametric part(FPM) and the convex hull for output decision

3 Experimental

3.1. Materials

Precursor fibers were prepared from homopolymeric polyacrylonitrile. The spinning solution was heated to 70 °C and a spinneret with 70 µm holes was used for the fiber production. The coagulation bath for precipitation contained a solution of 14 % resp. 19 % water and 86 % resp. 81 % dimethylformamide (DMF) with a temperature of 15 °C. There the fibers were stretched to a total draw ratio of four.

Table 1 Spinning parameters for the used precursor fibers

parameters	**value**
precursor fiber	PAN
mass ratio coagulation bath [wt.-%]	14/86 resp. 19/81
stretching ratio [-]	1:4
spinning temperature [°C]	70
titer [tex]	190

3.2. Experimental Setup

The precursor fibers were stabilized in a continuous stabilization line consisting of four HZs at temperatures ranging from 180 °C to 290 °C. The fibers were passed through each HZ several times, requiring a total process time of 120 min. The stretching was varied only in HZ 1, as this is, where the greatest influence on the process is to be expected, due to the interaction of physical fiber shrinkage and applied force [9, 23]. Three processes were carried out with stretching values of -0.28 %, 1.07 % and 3.60 % in the first heating zone. Following each process, samples were taken before the first heating zone and after each heating zone pass, resulting in a total of 28 samples per process.

3.3. Analysis

The relative cyclization index is determined by fourier transform infrared attenuated total reflectance (FTIR ATR) spectroscopy [24], where the absorption peaks A for C=N and C≡N bonds are evaluated according to Eq. (6).

$$RCI = \frac{A_{1580\,(\mathrm{C=N})}}{A_{1580\,(\mathrm{C=N})} + A_{2244\,(\mathrm{C\equiv N})}} \times 100\,\% \qquad (6)$$

The fiber density is measured via flotation method (DIN 65569). The fiber sample is suspended in a solvent mixture and by adding fluids with low or high densities (acetone, dibromomethane) an equilibrium state is set. By weighing this mixture at a known volume, the density can thus be calculated by dividing the mass by the volume.

4 Results and Discussion

4.1. Cyclization Progress

The RCI is dependent from process temperature and residence time, as these are the parameters with most influence on the cyclization progress [21]. With respect to the stretching in the HZs during stabilization, the *RCI* shows little dependence. All three tests have in common the initial decrease of the *RCI* in HZ 1 as can be seen in Fig. 3. Even after HZ 2, the RCI is still quite similar for different fiber stretching, although the differences in stretching are greatest in the first two HZs. Accordingly, there is no direct influence, at least at the selected process temperature. Upon entering HZ 3, the first

differences can be identified, see Fig. 3. The fiber, which had a free physical shrinkage behavior (0.89 % total stretching) in HZ 1, shows now a faster cyclisation reaction compared to the fiber with higher total stretching shown by the jump in HZ 3. This is likely related to the increased diffusion of oxygen into the

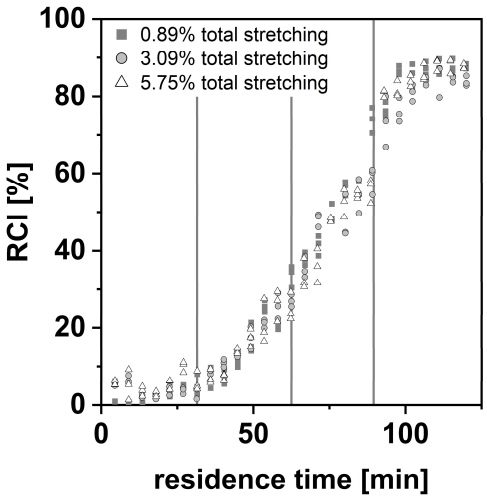

Figure 3 Measured RCI over residence time for different stretching, vertical lines representing HZs

fiber core [25]. The enhanced oxygen diffusion is usually reduced due to the enhanced formation of cyclized ladder polymer in the fiber sheat [26]. By an increased physical shrinkage, the polymer chains become less oriented in the fiber direction [27] and this seems to facilitate the oxygen diffusion. As a result, the enhanced oxygen concentration in the core can activate cyclization, but this effect decreases with increased stabilization residence times [22].

4.2. Density Progress

The density instead of RCI shows clear differences between the different stretching, see Fig. 4. Therefore, as temperature and residence times are quite similar, the density development is depending on fiber

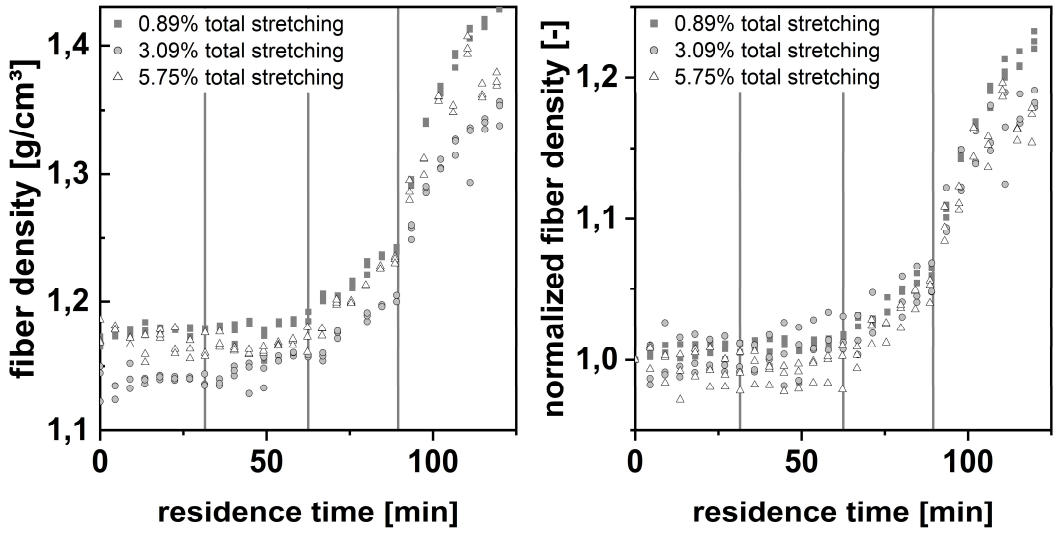

Figure 4 Measured fiber density (left) and fiber density normalized (right) with the precursor density for better comparison

precursor and the stretching parameter. The difference in density change is most evident in the last two HZs. Due to less inhibited diffusion, more oxygen reacts in the fiber core and thus an increased change in mass could be caused by oxygen accumulation. Additionally, it can be seen, that with reduced fiber

stretching in HZ 1 and HZ 2 the fiber density increases after stabilization, see Fig. 4. The difference between the tests with total stretching of 3.09 % and 5.75 % is not so evident, since the fiber density of one precursor fiber was lower than that of the other two used. This is probably related to a slight difference in concentration in the coagulation bath during spinning. With minimal stretching of 0.89 %, the density increases by about 22 % compared to the precursor, while increases of only 18 % and 15 % are evident in the other two tests. In addition to the change in mass, the fiber volume has an influence on this target parameter. Accordingly, the development of fiber length and diameter should be included in the consideration. Stretching and shrinkage are responsible for the change in fiber geometry. By no or negative stretching of the fiber, the physical shrinkage is not resisted, then no or just a small diameter reduction can be expected. Positive stretching instead causes a tensile force on the fiber, resulting in creep effects [27]. In this process, the entangled polymer chains are oriented in the longitudinal direction of the fiber, causing elongation of the fiber and a decrease in fiber diameter. In this process, the creep has a viscoplastic character, and the change is thus irreversible [27]. Thus, positive stretching should result in an increase in density due to the decrease in volume. However, for the investigated fibers actually a decrease can be shown, see Fig 4. The missing density increase could be caused by an overall decrease of the mass per fiber length, since the same number of particles is distributed over a larger fiber section when the diameter shrinks.

In HZ 2 with temperatures of 235 °C chemical shrinkage dominates over the physical shrinkage [9], as a result of increasing cyclization reaction. The thereby increased polymer crosslinking results in the shortening of the fiber length [27]. With the beginning of the oxidation of the PAN fiber in HZ 3 at 255 °C, the increase of the fiber density is evident. Whereupon in the HZ 4, the oxidation is significantly accelerated by the temperature jump from 255 °C to 290 °C [22], which leads to an increase of the mass-related density rise. Since the stretching was selected very similarly in HZ 3 and HZ 4, the chemical shrinkage in these zones should have a comparable effect. Accordingly, the density change would only depend on the mass change due to oxygen addition here.

Considering both, the stabilization progress, and the density of the fibers, it can be concluded that allowing physical shrinkage in the HZs should be prevented. Since this shrinkage accelerates the stabilization by a maximum of ten minutes in comparison to higher fiber stretching in HZ 1, see Fig 4. In return, however, the increased accumulation of oxygen is accepted. This will result in fibers with lower mechanical properties, since more carbon is outgassed in the form of carbon monoxide and carbon dioxide during carbonization, which will weaken the fiber structure as a result of the formation of voids and defects [28]. Thus, in order to optimally stabilize fibers, accurate modeling would be advantageous.

4.3. Model Validation

While training of the hybrid model the Levenberg-Marquardt algorithm was used for optimization. The validation was performed following the leave-one-out-cross validation. In case of fiber density, the principal progress over the stabilization process is qualitatively sufficiently represented, see Fig. 5. Whereas, for the fiber with 0.89 % stretching, the approximation is significantly lower than the measured data. In case of *RCI*, the approximate solutions look quite accurate in HZ 1 and HZ 2. While in HZ 3 the approximation for the 0.89 % stretching deviates, which is related to the ANN that shows severe difficulties in this area probably caused by a larger gap between the data points in the identification sets. This circumstance should be remedied with an increased number of data points in future studies. Looking at the parity plots in Fig. 6, the lack of accuracy of the hybrid model in the density calculation becomes clear. Especially for HZ 4 there is a wide spread comparing measured and computed density values. At the same time, it should be mentioned that for the approximation of the values in HZ 4, the stretching of HZ 1 was used, since the influence of this cannot be ignored, following the measurement results in Fig 4. That's why the hybrid model ignores the stretch in HZ 4 at the moment, this may be changed in future versions.

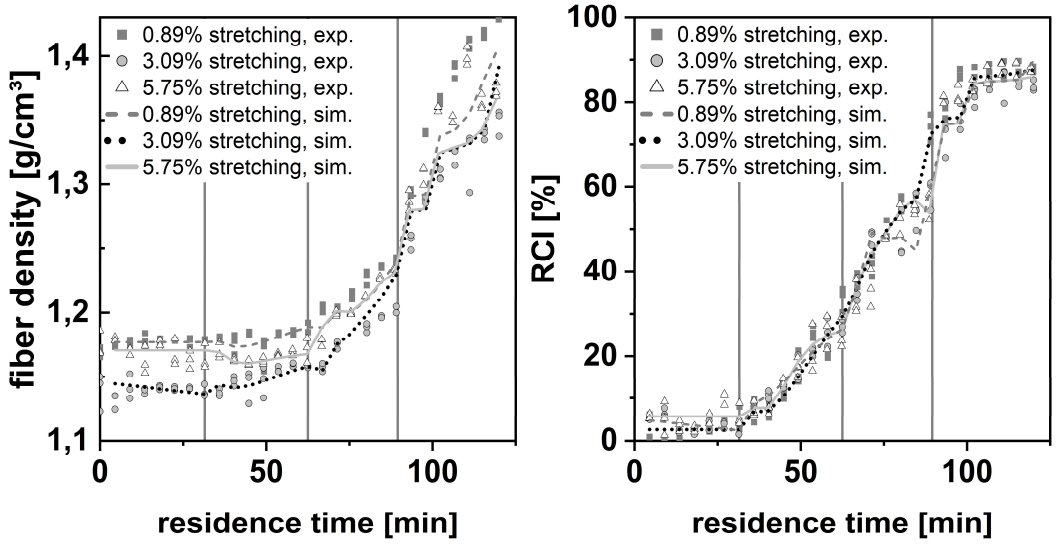

Figure 5 Measured (exp.) and simulated (sim.) values for density and RCI. The verticals represent the four HZs

The implementation as it exists to date continues to make allowances for the density outliers in HZ 4. It can be seen that black-box approaches often require large amounts of data to achieve satisfactory accuracy in prediction. This work shows the proof of concept, that for small data sets, already grey-box models can be developed. Still the model is limited to this data sets and needs to be increased in future studies. Since only the stretching in the first two HZs was significantly varied, the hybrid model is not expected to give accurate results for changing temperatures, residence times or stretching outside the

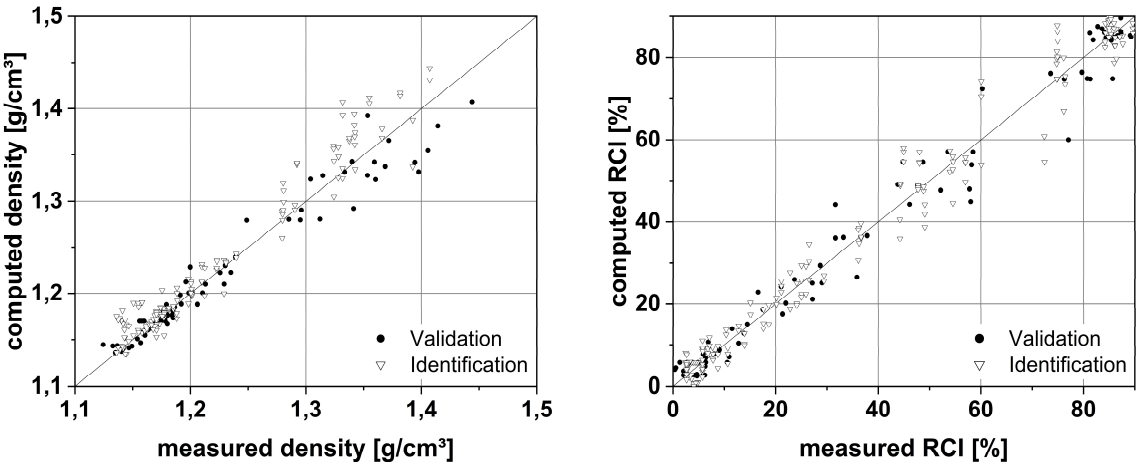

Figure 6 Parity plots for identification and validation of fiber density and RCI

selected ranges. However, the results so far are quite promising after all, as they show the possibilities for grey box modeling with mechanical and chemical model parts.

Future studies with more data sets will improve the proposed hybrid model. All input parameters should be varied individually in different experiments to incorporate their influence on stabilization into the model. In particular, stretching influence on the density development will be investigated in HZ 3 und HZ 4. Furthermore, the parametric approach should be extended with detailed stretching ratios of the different HZs instead of focusing on complete stretching ratios. Additionally, the calculation of the *RCI* should be used as input parameter similar to the fiber density. At last, the description of a changing diameter as a result of different stretching and shrinking phenomena will allow the development of precise white-box models, which will increase the extrapolation potential of the hybrid model. [29]

5 Summary and conclusion

In this paper, a hybrid semi-parametric model for a continuous stabilization process of CF was demonstrated to predict the stabilization progress as well as the fiber density. For this purpose, the parametric model part is based on the kinetics of chemical reaction and takes into the influence of

mechanical stress on the fiber by fiber stretching as input parameter account for the first time. In addition, an artificial neural network was created and trained to act as a black-box approach for the hybrid model. For validation of the hybrid model, three stabilization processes were carried out in which the stretching was varied in two of four HZs, while dwell time and process temperatures were kept constant.

For future studies it is recommended to integrate more data sets with broad process parameter windows by temperature, residence time and stretching to enhance the accuracy of the parametric model. Additionally, the parametric part should be extended for the transforming fiber diameter along the stabilization progress. The further improvement of the hybrid model will offer a faster way to develop tailored CF for individual purposes with less experimental costs.

Symbols used

A	[ ]	absorption intensity
D	[-]	empirical factor for change of fiber diameter
E_a	[J mol^{-1}]	energy
ΔH	[J mol^{-1}]	reaction enthalpy
M	[mol]	molar mass
RCI	[%]	relative cyclisation index
V	[cm^{-3}]	volume of solvent mixture
V_R	[m³]	reactor volume
$\dot{V}$	[m min^{-1}]	volume flow
c	[mol m^{-3}]	concentration
d	[m]	diameter
k	[min^{-1}]	rate constant
m	[g]	mass of solvent mixture
$\dot{m}$	[g min^{-1}]	mass flow
$\dot{n}$	[mol min^{-1}]	mass of substance flow
r	[mol min^{-1} m^{-3}]	reaction velocity
u	[m min^{-1}]	fiber transport velocity

Greek letters

ε	[%]	fiber stretching
ρ	[g cm^{-3}]	fiber density
τ	[min]	residence time

Sub- and Superscripts

e	input value before the first heating zone

Abbreviations

ANN	artificial neural network
C	carbon
CF	carbon fiber
FTIR ATR	fourier transform infrared attenuated total reflectance
FPM	first principle method
H	hydrogen
HZ	heating zone
N	nitrogen
PAN	polyacrylonitrile

References

[1] S. Soulis, G. Konstantopoulos, E. P. Koumoulos und C. A. Charitidis, *Fibers* **2020**, 8 (6), 33. DOI: 10.3390/fib8060033
[2] Y. Liu, Y. Xue, H. Ji und J. Liu, *J. Appl. Polym. Sci.* **2020**, 137 (24), 48819, DOI: 10.1002/app.48819
[3] Y. Liu und S. Kumar, *Polymer Reviews* **2012**, 52 (3), 234–258. DOI: 10.1080/15583724.2012.705410
[4] B. M. Terra, D. A. de Andrade und R. N. de Mesquita, *Polymer Testing* **2021**, 100, 107238. DOI: 10.1016/j.polymertesting.2021.107238
[5] R. Kraft, A. Kahnt, O. Grauer, M. Thieme, D. S. Wolz, D. Schlüter, M. Tietze, M. Curbach, K. Holschemacher, H. Jäger und R. Böhm, *Materials (Basel)* **2022**. DOI: 10.3390/ma15041619
[6] R. Böhm, M. Thieme, D. Wohlfahrt, D. Wolz, B. Richter und H. Jäger, *Fibers* **2018**, 6 (3), 56. DOI: 10.3390/fib6030056
[7] J. Li, Y. Yu, H. Li und Y. Liu, *J. Appl. Polym. Sci.* **2021**, 138 (38), 50988. DOI: 10.1002/app.50988
[8] J. Mädler, B. Richter, D. S. J. Wolz, T. Behnisch, R. Böhm, H. Jäger, M. Gude und L. Urbas, *Chemie Ingenieur Technik* **2022**, 94 (6), 889–896, DOI: 10.1002/cite.202100072
[9] E. Fitzer, A. K. Fiedler und D. Jürgen, *Chemie Ing. Techn.* **1971**, 43 (16), 923–931. DOI: 10.1002/cite.330431607
[10] M. Haghgoo, R. Ansari und M. K. Hassanzadeh-Aghdam, *Composites Part B: Engineering* **2019**, 167, 728–735. DOI: 10.1016/j.compositesb.2019.03.046
[11] M. Hao, X. Qian, Y. Zhang, J. Yang, C. Li, H. Gong, X. Wang, P. Wang, L. Liu und Y. Huang, *Composites Science and Technology* **2023**, 231, 109800. DOI: 10.1016/j.compscitech.2022.109800
[12] M. Sauer und D. Schüppel, „Market Report 2022 - The Global Market for Carbon Fibers and Carbon Composites," **2023**
[13] E. Frank, L. M. Steudle, D. Ingildeev, J. M. Spörl und M. R. Buchmeiser, *Angew. Chem.* **2014**, 126 (21), 5364–5403. DOI: 10.1002/ange.201306129
[14] H. Zhou, Y. Su, J. Zhang, H. Li, L. Zhou und H. Huang, *Chemical Engineering Journal* **2023**, 454, 140222. DOI: 10.1016/j.cej.2022.140222
[15] E. P. Koumoulos, A.-F. Trompeta, R.-M. Santos, M. Martins, C. M. d. Santos, V. Iglesias, R. Böhm, G. Gong, A. Chiminelli, I. Verpoest, P. Kiekens und C. A. Charitidis, *J. Compos. Sci.* **2019**, 3 (3), 86. DOI: 10.3390/jcs3030086
[16] H. Khayyam, R. N. Jazar, S. Nunna, G. Golkarnarenji, K. Badii, S. M. Fakhrhoseini, S. Kumar und M. Naebe, *Progress in Materials Science* **2020**, 107, 100575. DOI: 10.1016/j.pmatsci.2019.100575
[17] H. Khayyam, M. Naebe, O. Zabihi, R. Zamani, S. Atkiss und B. Fox, *IEEE Trans. Ind. Inf.* **2015**, 11 (4), 887–896. DOI: 10.1109/TII.2015.2434329
[18] J. Hofele, G. Link und J. Jelonnek, *Materials (Basel)* **2022**, 15 (3). DOI: 10.3390/ma15031222
[19] G. Golkarnarenji, M. Naebe, K. Badii, A. S. Milani, R. N. Jazar und H. Khayyam, *Computers & Chemical Engineering* **2018**, 109, 276–288. DOI: 10.1016/j.compchemeng.2017.11.020
[20] N. Shirolkar, P. Patwardhan, A. Rahman, A. Spear und S. Kumar, *Carbon* **2021**, 174, 605–616. DOI: 10.1016/j.carbon.2020.12.044
[21] A. L. Wilde, D. L. J. Alexander, A. P. Pierlot, R. Denning und M. Miao, *Fibers Polym.* **2021**, 22 (12), 3241–3250. DOI: 10.1007/s12221-021-0011-4
[22] M. Heine, „Optimierung der Reaktionsbedingungen von thermoplastischen Polymer-Fasern zur Kohlenstofffaser-Herstellung am Beispiel von Polyacrylnitril", Ph.D. Thesis, Universität Karlsruhe, **1988**
[23] J. Simitzis und S. Soulis, *Polym. Int.* **2008**, 57 (1), 99–105. DOI: 10.1002/pi.2322
[24] J. S. Church und D. J. Evans, *J. Appl. Polym. Sci.* **1995**, 57 (13), 1585–1594. DOI: 10.1002/app.1995.070571306
[25] E. Fitzer und D. J. Müller, *Carbon* **1975**, 13 (1), 63–69. DOI: 10.1016/0008-6223(75)90259-6
[26] L. Kong, H. Liu, W. Cao und L. Xu, *Fibers Polym* **2014**, 15 (12), 2480–2488. DOI: 10.1007/s12221-014-2480-1
[27] S. Soulis, D. A. Dragatogiannis, G. Konstantopoulos und C. Charitidis, *Materials Today: Proceedings* **2018**, 5 (14), 27645–27652. DOI: 10.1016/j.matpr.2018.09.085.

[28] T.-H. Ko, *J. Appl. Polym. Sci.* **1991**, 42 (7), 1949–1957. DOI: 10.1002/app.1991.070420719
[29] D. M. Dimiduk, E. A. Holm und S. R. Niezgoda, *Integr. Mater. Manuf. Innov.* **2018**, 7 (3), 157–172. DOI: 10.1007/s40192-018-0117-8